Journal of Wood Science

ORIGINAL ARTICLE

Open Access

# Compression properties of Japanese cedar (*Cryptomeria japonica*) treated with resin impregnation under loading perpendicular to the grain

Keita Ogawa[1*], Kenji Kobayashi[1] and Satoshi Fukuta[2]

**Abstract**

The compression properties of wood perpendicular to the grain is an important resistance mechanism in timber joints, especially wood-to-wood joints. Hence, improving the compression properties of wood is essential to developing timber joints with high resistance performance. In this study, we attempted to improve the compression properties using a resin impregnation technique. Three compression tests were conducted: loading at the full surface of the specimen, loading at the local part of the specimen with the unloaded part expanding in the tangential direction, and loading at the local part of the specimen with the unloaded part expanding in the longitudinal direction. Two types of resins were used: urethane and acryl. For compression loading on the full surface, the stiffness was increased by resin impregnation in the case of acryl impregnation. However, the yield load did not increase significantly. In the cases of compression loading in the local part and unloaded part expanding in the tangential direction, the stiffness increased when acryl was used, and the yield load increased when both resins were used. Significant increment in the properties were observed when the local compression load acted on the specimens with the unloaded parts expanding in the longitudinal direction. When urethane and a 10 mm incision depth were used, the stiffness and yield load increased 1.35 and 2.54 times, respectively. When using acryl and a 10 mm incision depth, the stiffness and yield load increased 1.64 and 2.93 times, respectively.

**Keywords** Compression perpendicular to the grain, Resin impregnation, Mechanical property

## Introduction

Wood is a well-known renewable energy resource and expanding its use is crucial for achieving sustainability. When using wood in construction, one of the main uses of wood, ensuring the safety of the construction against earthquakes and extreme weather events such as strong winds is necessary. Therefore, the development of engineering techniques to achieve this goal is desirable. During construction, several types of loading modes are applied to wooden members. Compression perpendicular to the grain is an important mechanical mode, particularly when moments are applied to wood-to-wood joints. Resistance against rotational force is generated at the contact area of the joints, and the characteristics of the joints are governed by the compression properties perpendicular to the grain [1–7]. Therefore, engineering techniques for improving the compression properties perpendicular to the grain are of interest for the development of wood-to-wood joints with high-moment performance. Driven by this motivation, Suesada et al. [8,

*Correspondence:
Keita Ogawa
ogawa.keita@shizuoka.ac.jp
[1] College of Agriculture, Academic Institute, Shizuoka University, 836 Ohya, Suruga-ku, Shizuoka 422-8529, Japan
[2] Aichi Center for Industry and Science Technology, 1261-1 Akiai, Yakusa, Toyota, Aichi 470-0356, Japan

9] attempted to improve the moment performance of a Nuki joint by attaching hardwood pieces to the contact area. They reported an improvement in the yield moment when Shirakashi wood was attached to a Nuki member. Chang et al. [10] attempted to insert a hardwood strip into the groove to improve the mechanical properties of planked timber shear walls in traditional Taiwanese buildings.

Wood is a cellular solid with pore spaces within its cells. When a compressive load acts on the wood, the cells are crushed, and the pore space is squeezed out. Therefore, the compression properties can be improved by preventing cell crushing. The authors focused on the resin impregnation technique developed by Fukuta et al. [11]. This technique consists of two processing stages: a microscopic incision on the wood surface is created with an ultraviolet (UV) wavelength short-pulse laser and resin is impregnated into the wood cell from the incision. It is expected that wood cells will not be crushed once they are filled with resin. An additional advantage is that the resin impregnation technique can be applied to arbitrary areas on the wood surface. For wooden joints, the area where the compression load acts under the rotational deformation of the joints can be predicted from the joint geometries. Therefore, it is sufficient to impregnate the resin even in the specific local specific area of the wood member to implement this technique. This leads to merits such as a reduction in the amount of resin and treatment work.

The authors previously attempted a resin impregnation technique to improve the mechanical properties of timber joints. In the case of the bolted joint [12], the resin was impregnated in the vicinity of the bolt hole. The lateral loading test results revealed that the bolted joint specimens treated with resin impregnation showed improvements in the initial stiffness and yield load compared to the non-treated specimen. For the screwed joint [13], the resin was impregnated in the vicinity of the screw. The lateral loading test results revealed that resin impregnation treatment improved the initial stiffness. The authors also investigated the effects of resin impregnation on the embedment properties loaded by a round bar [14]. Embedment tests revealed improvements in the initial stiffness and yield load.

In the case of compression perpendicular to the grains, most of the deformation can be expressed as cell crushing. The authors expected that the resin impregnation technique would also be effective in improving the compression properties. In this study, a resin impregnation technique was applied on the wood specimen for improving the compression properties perpendicular to the grain. Small clear specimens were prepared, compression tests were conducted with the resin-impregnated specimens, and the characteristics were compared with those of the non-treated specimens.

## Materials and methods

### Material preparation

Forty solid air-dried pieces of Japanese cedar (*Cryptomeria japonica* D. Don) were prepared. The moisture content was measured in the non-resin-impregnated specimens after testing. Average and standard deviation was 11.0 ± 0.6%. The dimensions of the pieces were 120 × 30 mm in the cross-section and 230 mm in the longitudinal direction. The pieces do not have any knots or remarkable splits. First, the densities of the pieces were measured. The pieces were divided into five groups to minimize the difference in density between the groups. The average and standard deviations of the density are listed in Table 1. Three specimens were prepared from each piece, as described later.

Next, microscopic incisions were made on the surfaces of the pieces using a UV laser. Diode-pumped solid-state Q-switched lasers (Spectra-Physics, Talon355-15SH) were used in this study. The pattern shown in Fig. 1 was drawn with a hole density of 667 holes/cm$^2$ using a Galvano scanner. The target incision depth was set to 4 mm or 10 mm. The laser irradiation parameters in this study,

**Table 1** Summary of the testing groups

| Group | *n*[a] | Density[b] (kg/m$^3$) | Resin | Incision depth (mm) | Testing method |
|---|---|---|---|---|---|
| N-F | 8 | 353.4 ± 22.0 | None | — | F[c] |
| N-LT | 8 | | None | — | LT[d] |
| N-LL | 8 | | None | — | LL[e] |
| U4-F | 8 | 353.6 ± 19.4 | Urethane | 4 | F |
| U4-LT | 8 | | Urethane | 4 | LT |
| U4-LL | 8 | | Urethane | 4 | LL |
| U10-F | 8 | 353.6 ± 19.9 | Urethane | 10 | F |
| U10-LT | 8 | | Urethane | 10 | LT |
| U10-LL | 8 | | Urethane | 10 | LL |
| A4-F | 8 | 353.2 ± 17.9 | Acryl | 4 | F |
| A4-LT | 8 | | Acryl | 4 | LT |
| A4-LL | 8 | | Acryl | 4 | LL |
| A10-F | 8 | 353.3 ± 15.8 | Acryl | 10 | F |
| A10-LT | 8 | | Acryl | 10 | LT |
| A10-LL | 8 | | Acryl | 10 | LL |

[a] *n*: number of specimens

[b] The values of mean average ± standard deviation

[c] F: compression load acting on the full surface

[d] LT: compression load acting on the local part of the surface with the unloaded part expanding in the tangential direction

[e] LL: compression load acting on the local part of the surface with the unloaded part expanding in the longitudinal direction

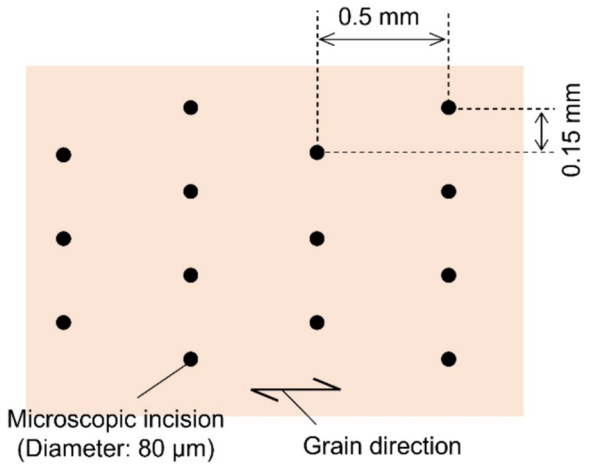


**Fig. 1** Incision pattern

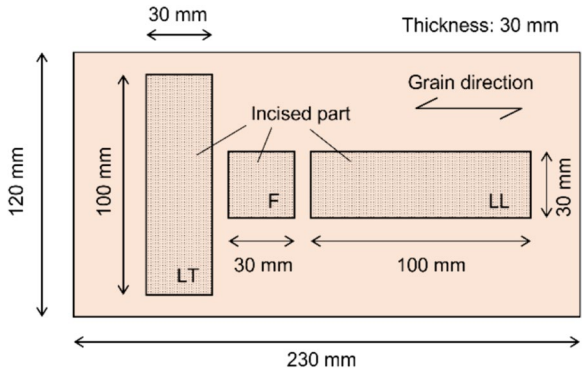


**Fig. 2** Incisions on a wood piece

listed in Table 2, were the same as those in our previous studies [12–14]. An incision was made on the dotted parts of the surfaces of the wood pieces, as shown in Fig. 2. The dimensions of the parts with symbols F, LT, and LL were 30 (L)×30 (T) mm, 30 (L)×100 (T) mm, and 100 (L)×30 (T) mm, respectively.

Finally, the resin was impregnated into the wood pieces. Two types of resins were used in this study, which were identical to those used in our previous studies [12–14]. The first was a urethane prepolymer (Kotobukikakou Co., Ltd., PS-NY6) (hereafter, urethane). The urethane evaporation residue was approximately 40%. The second resin is an acrylic monomer (Toeikasei Co. Ltd., DIAKITE PF-2730) (hereafter, acryl). 0.6 parts by weight of 2,2'-azobisisobutyronitrile was used as a polymerization initiator. A pipette is used to impregnate the resin. The liquid-type resins were dropped onto the incision and allowed to be absorbed into the wood. This process was continued until full impregnation was achieved. Because urethane is a cold-setting polymer, the wood pieces were left to stand for over 1 week after impregnation for curing. Since acryl polymerizes in an anaerobic environment, a heating press machine was used with a temperature of 140 ℃ but with no pressure applied, such that only the surface of the wood piece touched the heating plate of the machine. The heating duration was approximately 30 min. Unlike the previous impregnation conducted by Yano [15], the molecular weights of the resins used in this study were sufficiently high, and the absorption of the resin into the wood cell wall seemed limited. Therefore, this study mainly focused on what occurs when wood cells are filled with resin under a compression load perpendicular to the grain.

**Table 2** Laser irradiation parameters

| | Target depth | |
|---|---|---|
| | 4 mm | 10 mm |
| Wavelength (nm) | 355 | 355 |
| Pulse width (ns) | 25 | 25 |
| Pulse energy (μJ) | 260 | 260 |
| Pulse repetition rate (kHz) | 50 | 50 |
| Power (W) | 13 | 13 |
| Theoretical focal spot diameter (μm) | 22.6 | 22.6 |
| Irradiation time per hole (ms) | 3 | 20 |

### Specimen preparation and testing method

After curing, the pieces were cut into specimens. Pieces were cut along the sides of the incised parts. The specimen with symbol F was used for the compression test loading to the full surface, as shown in Fig. 3a. The specimens were set to ensure that the impregnated part was placed on the upper surface. A specimen with symbol LT was used for the compression test loading on the local part with the unloaded part expanding in the tangential direction, as shown in Fig. 3b. A specimen with symbol LL was used for the compression test loading on the local part with the unloaded part expanding in the longitudinal direction, as shown in Fig. 3c. The setup of the locally loaded tests was determined according to the report written in Tanahashi et al. [16]. Even in the case of the LL setup, it seems to have a sufficient length at the unloaded part for involving the stiffness increment, owing to the deformation occurring in this part. All the specimens were loaded in the radial direction.

Compression tests were conducted using a universal testing machine (AG-I 250 kN, Shimadzu Co. Ltd.). A continuous downward load of 3.0 mm/min was applied to the specimens through the steel plate. The relationship between the load and deformation was measured during the test. The load was measured using a load cell (SFL-50kNAG; Shimadzu Co., Ltd.). Two displacement

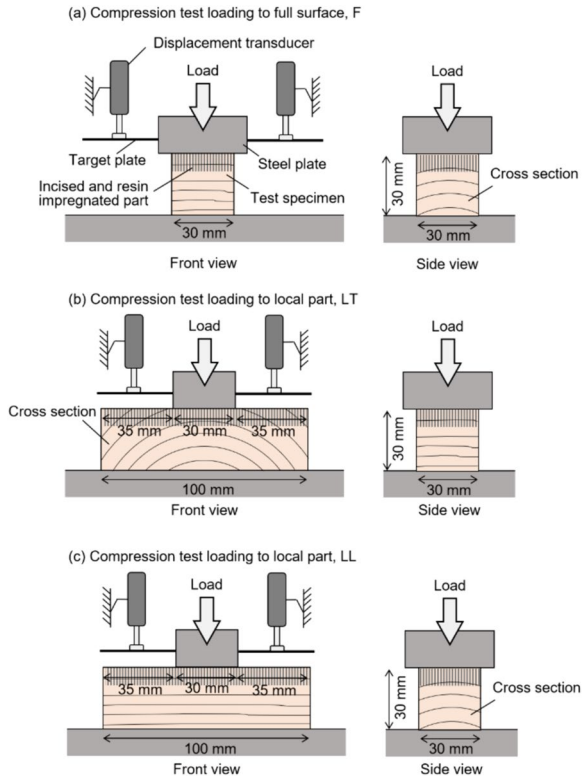


**Fig. 3** Testing setup

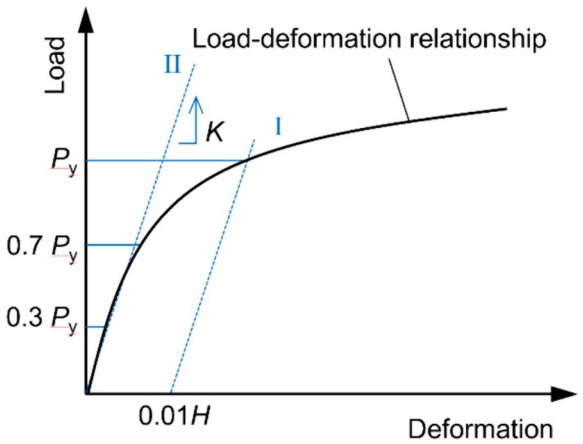


**Fig. 4** Derivation method for yield load and stiffness

transducers (CDP-25, Tokyo Measurement Instruments Laboratory Co., Ltd.) were attached to measure the deformations of the specimens. The average of two read values obtained from the transducers was used as the deformation. The loading was continued until the deformation reached 20 mm or until the load reached 40 kN. Eight specimens were tested in each group. The specimen groups are listed in Table 1.

### Characteristics derivation

The characteristics were derived based on the relationship between load and deformation. In this study, yield load $P_y$ and stiffness $K$ were determined. The derivation method, shown in Fig. 4, was as follows. First, a linear regression was conducted on the range of elastic behavior observed around an original point. The regression range was visually determined. The line was offset to rightward at 0.01$H$, where $H$ is the height of the specimen ($H$=30 mm). This line is referred to as Line I in Fig. 4. The intersection of Line I and the relationship was determined to be the yield point, and the load at this point was the yield load, $P_y$. Next, the data plots in the range between 0.3$P_y$ and 0.7$P_y$ were linearly regressed, and the line was named Line II. Then, the least squares method was used for regression. The slope of Line II was determined as stiffness $K$.

The characteristics of most specimens were obtained using this method. However, two specimens (one from group A4-LT and one from group A10-LT) were not suitable for this method. An obvious difference was observed between the slopes of Line II and this relationship. For these specimens, the regressed data range for Line II was changed to 0.3$P_y$ and 0.6$P_y$, resulting in a smaller difference between the slopes. The stiffness values of the two specimens are included in the results presented in the following section.

## Results and discussion

### Relationship between load and deformation

Examples of the relationships between the load and deformation are shown in Fig. 5. The figure shows one example for each group, and the data shown are for the specimens that had the fourth-highest yield load among the eight in each group.

Figure 5(a-1),(a-2) shows the results of the compression test loading on the full surface (loading mode F); the same test data are shown in both graphs. However, the ranges of the axes are different. (a-1) shows the entire set of test data, and (a-2) focuses on the data at the beginning of the test. As shown in Fig. 5(a-2), the test results showed linear relationships. The yielding behavior began at approximately 3 kN, and a plateau behavior was observed after yielding. At large deformations, the load increased again. This behavior is well known as a typical behavior in cellular solids and so called "densification" [17]. When the deformation reached a large value, the pore space in the wood cells was sufficiently squeezed out and the compressive resistance increased. In groups N-F, densification

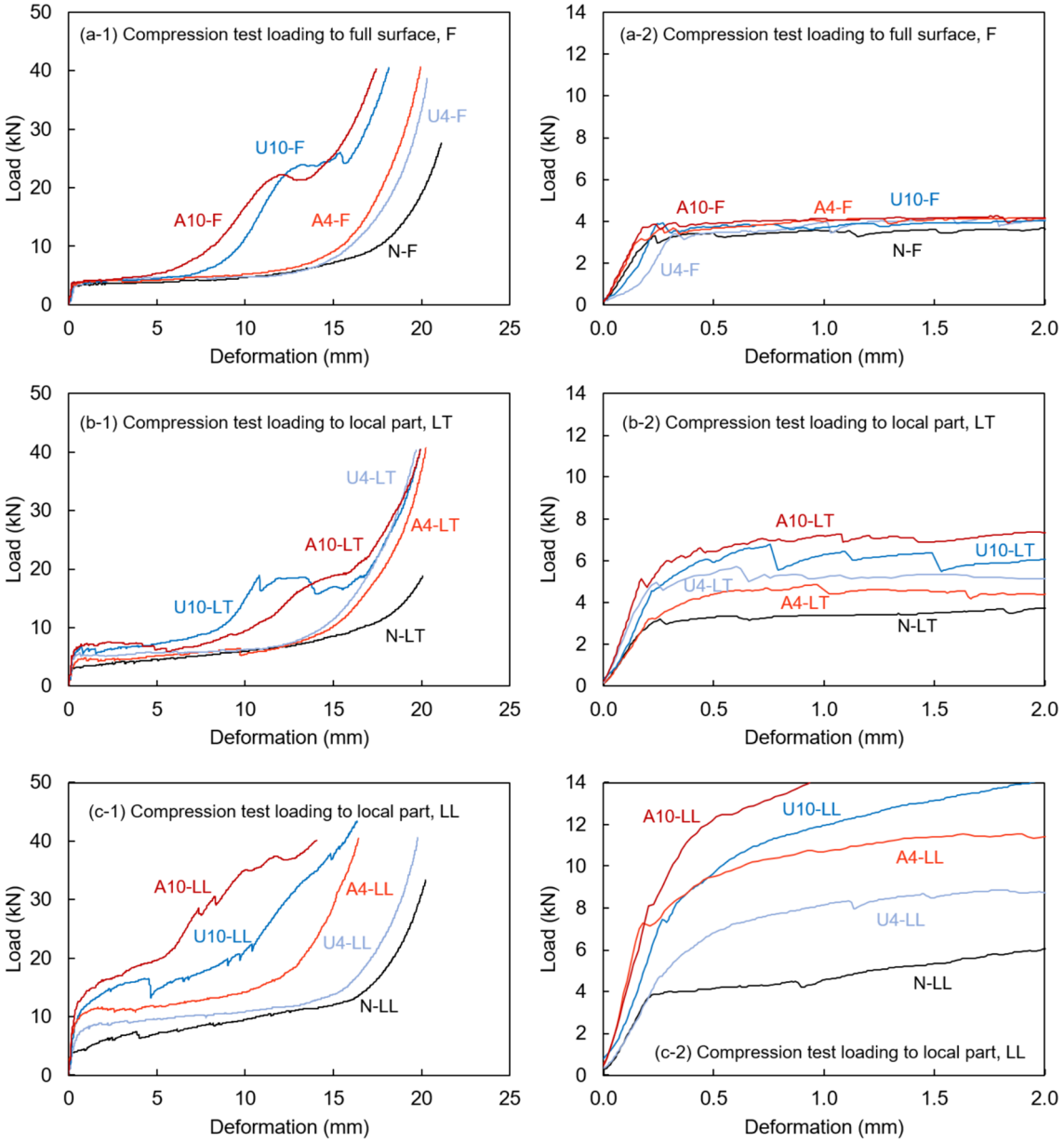


**Fig. 5** Examples of relationships between load and deformation. The graphs with "-1" show the whole data and the graphs with "-2" show focused data around the beginning of the test

started at a deformation of approximately 18 mm. In the case of the resin-impregnated groups with an incision depth of 4 mm (U4-F and A4-F), densification started with a smaller deformation. In the case of the resin-impregnated groups with an incision depth of 10 mm (U10-F and A10-F), densification started at approximately 7–8 mm, which was much smaller than that for the other groups. These results implied that the pore space in the wood cells was reduced by resin impregnation. Figure 5(a-2) shows the effect of resin impregnation on the compression properties, and the details are discussed in the next section.

The compression test results when loading to the local part are shown in the other graphs in Fig. 5. Figure 5(b-1), (b-2) shows the cases in which the unloaded parts expanded in the tangential direction (loading mode LT), and Fig. 5(c-1), (c-2) shows the cases in which the unloaded parts expanded in the longitudinal direction (loading mode LL). In all specimens, similar behaviors were observed in the case of loading mode F, which

indicated elastic linear behavior, plateau behavior after yielding, and densification at large deformations. When wood was loaded with mode LL, two features appeared: a higher resistance than mode F and a slight increment in load after yielding. A higher resistance occurs because of the deformation of the unloaded parts, as illustrated in Fig. 6. Additional energy is required to deform the unloaded parts, and the resistance increases as a result. The slight increment in load after yielding is conceivable through the following mechanism: under local compression, deformation occurred in the unloaded part, and the shape became an exponential curve [18–20]. Even when the deformation at the loaded part increases, elastic deformation still occurs at a point at a considerable distance from the loaded part, as indicated by the blue arrow.

In Fig. 5(c-1), a slight increase in the load after yielding is clearly observed. Slight increases were also observed in U4-LL and A4-LL, but the slope was smaller than that in N-LL. It is assumed that the upper part of the resin-impregnated specimens became brittle, and microcracks appeared. Subsequently, discontinuous surface deformation occurred, and the deformation at the unloaded part decreased. Although the load of the resin-impregnated specimens also slightly increased after yielding, a reduction due to brittleness occurred simultaneously. Consequently, U4-LL and A4-LL exhibited smaller slopes after yielding. For U10-LL and A10-LL, a rapid increase in densification was observed. Therefore, it is difficult to discuss the slope that appears after yielding. In the case of mode LT, the increase after yielding was smaller than that in the case of LL. This behavior was observed in all specimens, regardless of whether the resin was used.

### Characteristics of the specimen loaded to full surface

The averages and standard deviations of the stiffness are shown in Fig. 7. The stiffness of N-F was 15.1 ± 2.4 kN/mm. When the value is translated to the Young's modulus by dividing the load by the compression area and dividing the deformation by the height of the specimen, it becomes 503.4 ± 79.7 MPa. The stiffness of U4-F was 13.8 ± 3.3 kN/mm, which was lower than that of group N-F. The stiffness of U10-F was 16.1 ± 5.6 kN/mm, which was almost equal to that of N-F. Although groups U4-F and U10-F were the resin-impregnated groups, their stiffness did not increase. The stiffnesses of A4-F and A10-F were 19.4 ± 4.5 and 21.9 ± 4.2 kN/mm, respectively. In the case of acryl, an increase was observed. Dunnett's test was conducted to compare the average values of the non-impregnated and impregnated groups. The $p$ values of the N-F vs. U4-F and N-F vs. U10-F pairs were 0.919 and 0.970, respectively. This implies that the strengthening effect was negligible. The $p$ value of N-F vs. A4-F was 0.150, indicating no significant difference at the 10% significance level. The $p$ value of N-F vs. A10-F was 0.009, implying that a sufficient increment was observed.

In this study, a simple mathematical approach was adopted. The authors' previous study [14] reported a micro image obtained using a scanning electron microscope (SEM), and the resin-filled wood cells were less deformed under an embedment load. Based on this report, the authors assumed that the resin-impregnated part performed like a rigid part in loading mode F. With this assumption, the stiffness of the resin-impregnated part $K_r$ was derived using the stiffness of the non-resin-impregnated specimen $K_n$ (15.1 kN/mm), the height of

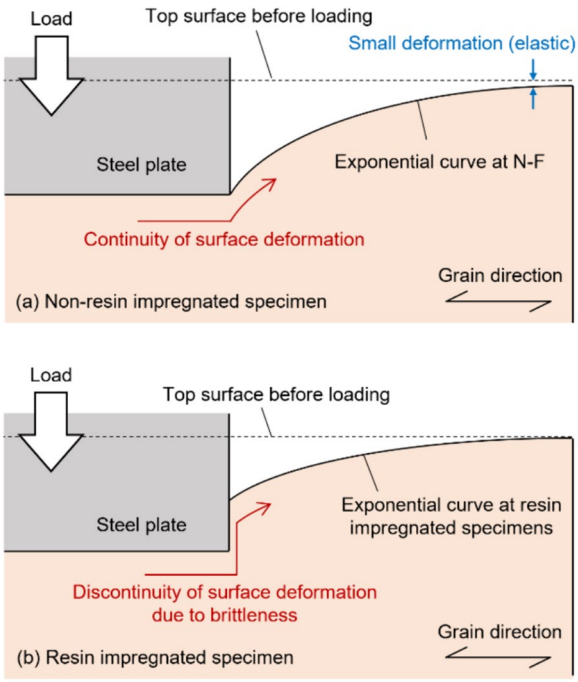


**Fig. 6** Images of deformation at the unloaded and loaded parts

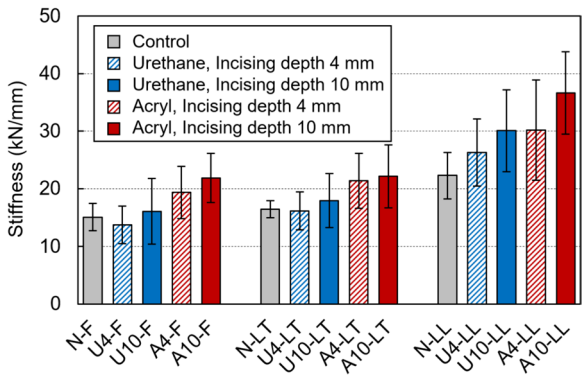


**Fig. 7** Average and standard deviation of stiffness

the specimen $H$ (30 mm), and the incision depth $D$ (4 or 10 mm).

$$K_r = K_n \cdot \frac{H}{H - D}. \quad (1)$$

Then, the value of $K_r$ in groups at incision depth of 4 mm was 17.4 kN/mm, and that at 10 mm was 22.7 kN/mm. When the calculated and average values of the test results were compared, the groups using acryl showed good agreement. This confirms the validity of this assumption. For urethane, the measured values were lower than the calculated values. This was considered to be influenced by the evaporation residue of urethane used in this study. The evaporation residue was approximately 40%, indicating that micro spaces existed after curing. According to reports by Totsuka et al. [21, 22] and Kobayashi and Ogawa [23], compressive stiffness is influenced by the roughness of the top surface. In the specimens using urethane, the micro space appeared and played a similar role to the roughness.

The average and standard deviations of the yield loads are shown in Fig. 8. The yield load of N-F is 3.38 ± 0.46 kN. The highest value was 4.24 ± 1.53 kN observed in group U10-F. In contrast to the stiffness, this increase was smaller. Analysis of variance (ANOVA) was conducted and the $p$ value was 0.227, indicating that a significant difference was not observed at a significance level of 0.05. The reason is that the yield load was determined by the weakest point in the specimen. Even in the resin-impregnated groups, the non-impregnated part existed under the incision depth and the weakest point existed in this non-impregnated part. Kambe [24] reported a similar result when attempting to improve the compression properties using long screws.

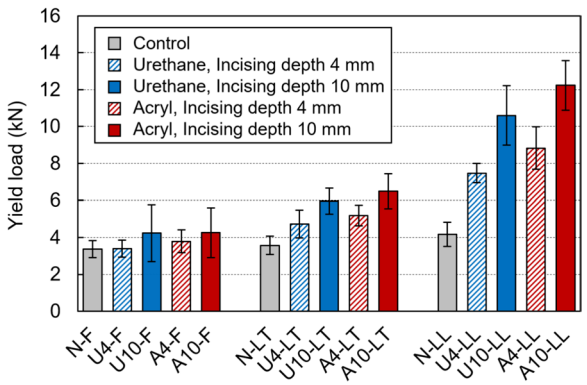


**Fig. 8** Average and standard deviation of yield load

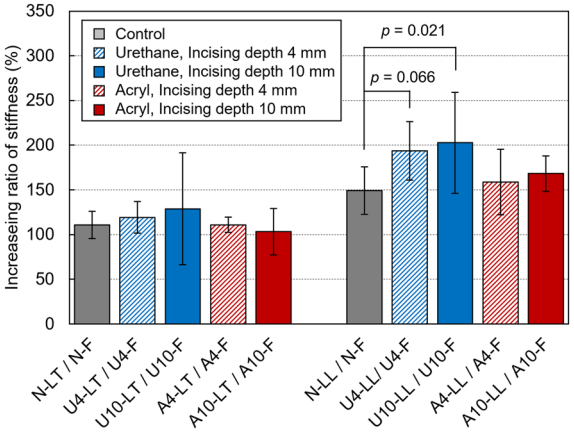


**Fig. 9** Increasing ratio of stiffness. $p$ values are the result of Dunnett test. $p$ values for non-described pairs were over 0.6

### Characteristics of the specimen loaded to the local part

The stiffness values of the specimens loaded onto the local part are shown in Fig. 7. The result of mode LT was similar to that of mode F; the specimens using urethane showed a smaller increment compared to the non-impregnated specimens, and the specimens using acryl showed a significant increment. In mode LL, the stiffness was increased by the resin impregnation. The stiffness of N-LL was 22.3 ± 4.0, and the stiffnesses of U4-LL, U10-LL, A4-LL, and A10-LL were 26.3 ± 5.6, 30.1 ± 7.1, 30.2 ± 8.7, and 36.6 ± 7.2 kN/mm, respectively. The ratios of the impregnated to non-impregnated specimens were 1.18, 1.35, 1.35, and 1.64, respectively. Dunnett's test was also conducted and their $p$ values were 0.588, 0.087, 0.081, and < 0.001. A significant difference was observed only in the N-LL vs. A10-LL pair at a significance level of 0.05. Although significant differences were not observed in the N-LL vs. U10-LL and N-LL vs. A4-LL pairs at this significance level, the differences were similar to those observed in the other pairs.

When the wood was locally loaded, a higher stiffness was observed owing to the occurrence of deformation at the unloaded parts. To examine this effect, it is effective to calculate the increasing ratio of the stiffness, which can be derived by dividing the stiffness of the specimen locally loaded by the specimen loaded to the full surface. In this study, the stiffness of the locally loaded specimen (modes LT and LL) was divided by that of the specimen of mode F obtained from the same wood piece, as shown in Fig. 2. The averages and standard deviations are shown in Fig. 9. The ratio of the non-impregnated group (N-LT/N-F) was 110.7 ± 15.2%. The impregnated groups showed a similar ratio, which implies that the resin impregnation had little effect on the stiffness increment in mode

LT. An ANOVA was conducted and the $p$ value was 0.574, which means that a significant difference was not recognized. In the mode LL, the ratio of the non-impregnated group (N-LL/N-F) was 149.2 ± 26.7%. The groups using urethane showed higher ratios, and the average and standard deviation of U4-LL/U4-F and U10-LL/U10-F were 193.7 ± 32.6 and 202.6 ± 56.4%, respectively. The higher ratios observed in these groups indicated that urethane impregnation effectively increased the stiffness ratio. The mechanism seems to be that the urethane in the wood cell helps transmit the load from the loaded part to the unloaded part, and the deformation in the loaded part becomes larger than that in the non-impregnated specimen. This study did not attempt to validate the mechanism; however, the method for measuring surface deformation using digital image correlation [25] may be helpful for its verification. In contrast, the stiffness ratio of the specimens using acryl did not increase. The average and standard deviation of A4-LL/A4-F and A10-LL/A10-F were 158.7 ± 36.6 and 168.1 ± 19.7%, respectively, which were almost equal to those for the non-impregnated groups. The reason for this is not clear, but it may influence the difference in the mechanical properties between urethane and acryl. Although it is difficult to understand the deformation behavior of resins restrained by wood cells, it is important to clarify it. Dunnett's test was conducted for mode LL, and low $p$ values were derived for the N-LL/N-F vs. U4-LL/U4-F and N-LL/N-F vs. U10-LL/U10-F pairs, which were 0.066 and 0.021, respectively. For the other pairs, the $p$ value was greater than 0.6.

The results of the yield load for the local loading cases are shown in Fig. 8. An increase in resin impregnation was observed in both the LT and LL modes. In mode LT, the non-impregnated specimen (N-LT) showed 3.57 ± 0.49 kN. The increasing ratios of U4-LT, U10-LT, A4-LT, and A10-LT, calculated by dividing the value of the impregnated specimen by that of the non-impregnated specimen, were 1.32, 1.67, 1.45, and 1.82, respectively. Comparing the results of LT and LL, LL showed higher strengthening than LT. Non-impregnated specimen (N-LL) showed 4.17 ± 0.65 kN. The increasing ratios of U4-LL, U10-LL, A4-LL, and A10-LL, which were calculated by dividing the value of the impregnated specimen by that of the non-impregnated specimen, were 1.79, 2.54, 2.12, and 2.93, respectively. When comparing the results of incision lengths of 4 and 10 mm, the results of the 10 mm incision showed higher strengthening. Although it takes more time to create the incision at a depth of 10 mm than at 4 mm (irradiation time in Table 2), a stronger effect can be obtained with incision at a greater depth.

## Conclusions

This study attempted to improve the compression properties of wood perpendicular to the grain using a resin impregnation technique. Two types of resins, two incision depths, and three loading modes were used. In the case of compression loading of the full surface, the stiffness was increased when acryl was used, but sufficient strengthening effect was not observed when urethane was used. The yield load was not sufficiently strengthened by resin impregnation. In the cases of compression loading in the local part and unloading expanding in the tangential direction, the stiffness increased when acryl was used. The yield load increased when both resins were used. When the local compression load acted on the specimens with the unloaded parts expanding in the longitudinal direction, high strengthening effect was observed, especially at an incision depth of 10 mm. When urethane and a 10 mm incision depth were used, the stiffness and yield load increased 1.35 and 2.54 times, respectively. When using acryl and a 10 mm incision depth, the stiffness and yield load increased 1.64 and 2.93 times, respectively.

This study mainly reports the strengthening effect quantitatively for a limited number of resin types. To achieve a higher strengthening effect, it is necessary to use more types of resin. In addition, to reveal the compression mechanism, it is important to understand the deformation behavior of the resin with wood cell restraint.

#### Abbreviations

| | |
|---|---|
| UV | ultraviolate |
| SEM | scanning electron microscope |
| ANOVA | analysis of variance |

#### Acknowledgements

This study was financially supported by the JSPS KAKENHI (grant number: 22K14925). The authors thank Mr. Nomura, a researcher at the Aichi Center for Industry and Science Technology, for his assistance with the operation of the UV laser machine. The authors also thank Ms. Endo, a bachelor's course student at Shizuoka University, for her help with specimen preparation and test conduction.

#### Author contributions

KO designed and performed the experiments and analyzed the data. SF advised to decide the processing conditions. KO wrote the manuscript in consultation with SF and KK. All the authors have read and approved the final manuscript.

#### Funding

This study was financially supported by the JSPS KAKENHI (grant number: 22K14925).

#### Availability of data and materials

All data discussed during this study are included in this published article.

## Declarations

#### Competing interests

The authors declare that they have no competing interests.

Received: 10 April 2024 Accepted: 31 May 2024
Published online: 06 June 2024

**References**

1. Chang WS, Hsu MF, Komatsu K (2006) Rotational performance of traditional Nuki Joints with gap I: theory and verification. J Wood Sci 52:58–62
2. Chang WS, Hsu MF (2007) Rotational performance of traditional Nuki Joints with gap II: the behavior of butted Nuki joint and its comparison with continuous Nuki joint. J Wood Sci 53:401–407
3. Ogawa K, Sasaki Y, Mariko Y (2015) Theoretical modeling and experimental study of Japanese "Watari-ago" joints. J Wood Sci 61:481–491
4. Ogawa K, Sasaki Y, Yamasaki M (2016) Theoretical estimation of the mechanical performance of traditional mortise-tenon joint involving a gap. J Wood Sci 62:242–250
5. He JX, Yu P, Wang J, Yang QS, Han M, Xie LL (2021) Theoretical model of bending moment for the penetrated mortise-tenon joints involving gaps in traditional timber structure. J Build Eng 42:103102
6. Tanahashi H, Ooka Y, Suzuki Y (2021) Rotational embedment mechanism of traditional wooden strut and its formulation. Japan Archi Rev 4(2):320–331
7. Ogawa K (2016) Mechanical analyses of traditional Japanese wooden joints. Mokuzai Kogyo 71(9):349–354 (**in Japanese**)
8. Suesada H, Miyamoto K, Shibusawa T, Aoki K, Inayama M (2019) Reinforcing effect of hardwoods on the moment resistance performance of traditional Japanese "nuki"-column joints. J Wood Sci 65:65
9. Suesada H, Miyamoto K, Shibusawa T, Inayama M, Aoki K (2020) Characteristic values of rotational moment resistance performance of a nuki-column joint reinforced with hardwood -Proposal of post-yield evaluation method and grasping relationships between the joint performance and compression perpendicular to the grain performance of the materials-. Bullet FFPRI 19(2):185–194 (**in Japanese**)
10. Chang WS, Hsu MF, Komatsu K (2011) A new proposal to reinforce planked timber shear walls. J Wood Sci 57:493–500
11. Fukuta S, Nomura M, Ikeda T, Yoshizawa M, Yamasaki M, Sasaki Y (2018) UV-laser incision to apply wood-plastic compositions to wood surface. Mokuzai Gakkaishi 64:28–36 (**in Japanese**)
12. Ogawa K, Fukuta S, Kobayashi K (2020) Experimental study of lateral resistance of bolted joints using Japanese cedar (*Cryptomeria japonica*) treated with resin impregnation. J Wood Sci 66:71
13. Ogawa K, Kobayashi K, Fukuta S (2023) Effect of resin impregnation into wood cell on lateral resistance of screwed joint connecting solid wood and steel plate. Proc WCTE2023, 1104–1109, Oslo, June 19–22
14. Ogawa K, Fukuta S, Kobayashi K (2022) Embedment properties of Japanese cedar (*Cryptomeria japonica*) treated with resin impregnation. J Wood Sci 68:9
15. Yano H (2003) Production of high strength wood-based materials. Mokuzai Kogyo 58(4):150–156 (**in Japanese**)
16. Tanahashi H, Ooka Y, Izuno K, Suzuki Y (2011) Yielding mechanism of embedment of wood and formulation of elasto-plastic embedment displacement. J Struct Constr Eng AIJ 76(662):811–819 (**in Japanese**)
17. Gibson LJ, Ashby MF (1997) The mechanics of foams: basic results. In: Cellular solids, 2nd edn. Cambridge: Cambridge University Press.
18. Inayama M (1993) Study on compression perpendicular to the grain in wood Part 4: Analytic functions for the relation between compression load and elastic deformation perpendicular to the grain in wood. Summaries of technical papers of Annual meeting AIJ, Tokyo, 907–908 (**in Japanese**)
19. Tanahashi H, Shimizu H, Suzuki Y (2006) Elastic surface displacements of orthotropic wood due to partial compression based on Pasternak model. J Struct Constr Eng AIJ 609:129–136 (**in Japanese**)
20. Tanahashi H, Shimizu H, Horie H, Yang P, Suzuki Y (2008) Elastic embedded displacements of orthotropic wood with a finite length based on Pasternak model. J Struct Constr Eng AIJ 73(625):417–424 (**in Japanese)**)
21. Totsuka M, Jockwer R, Kawahara H, Aoki K, Inayama M (2022) Experimental study of compressive properties parallel to grain of glulam. J Wood Sci 68:33
22. Totsuka M, Jockwer R, Aoki K, Inayama M (2023) Compressive stiffness parallel to grain in timber. Proc WCTE2023, 251–258, Oslo, June 19–22
23. Kobayashi K, Ogawa K (2022) Influences of surface roughness of borehole on embedment stiffness of timber. Summaries of technical papers of Annual meeting AIJ, Sapporo, 22086 (**in Japanese**)
24. Kambe W (2017) An experimental study on reinforcing embedment strength with long screws for glue laminated timber. Soc Sci Eng/Arch Environ Design Kanto Gakuin Univ 61:7–14 (**in Japanese**)
25. Kawano K, Aoki K, Inayama M (2023) Study on the shape of the additional area on partial compression perpendicular to the grain of large section glued laminated timber. Mokuzai Kogyo 78(5):176–182 (**in Japanese**)

## Publisher's Note